

# INFLUENCE OF PRESSURE ON THE INTERACTION BETWEEN ALUMINA – MULLITE SHELL MOULDS AND MOLTEN NICKEL ALLOYS

JAROSLAV CIHLÁŘ, KAREL MACA, PETER MARQUIS\*

*Institute of Materials Engineering, Department of Ceramics,  
Technical University of Brno, Technická 2, 616 69 Brno*

*\*University of Birmingham,  
Birmingham, Great Britain*

Received 13. 9. 1995

*The interaction of ceramic alumina-mullite mould with nickel and nickel alloys (ZhS6K, NiTi and NiCr) was studied at a temperature of 1773K in the pressure range from 0.1 to  $10^5$  Pa. The ceramic mould contained a continuous network of pores, which provided for the releasing of the gaseous phase at the mould(s)/metal(l) interface and thus facilitated physical and chemical erosion of the face layer of the mould at low pressures. Increasing the pressure of gaseous atmosphere to over  $10^4$  Pa practically prevented the erosion of mould surface by nickel and its alloys.*

## INTRODUCTION

Unidirectional solidification of refractory nickel alloy castings, which is most frequently carried out in vacuum, takes place under prolonged contact between molten alloys and ceramic shell moulds. This contact is accompanied by physical and chemical interactions of alloys with ceramic moulds and this may show in surface defects of castings [1]. The extent of interactions depends on the chemical composition of moulds and crystallized alloys, and on the physical conditions accompanying the interaction. The effect of pressure on physical and chemical events at the mould/alloy interface was not usually regarded as significant [2]. Interactions were observed only at reduced pressure in case of alloys containing carbon. Here, the formation of carbon dioxide takes place as the consequence of the reaction of carbon with ceramic mould [2,3].

Our earlier results have shown, however, that the effect of pressure on the extent of interactions between moulds and Ni-alloys is significant even when the alloys do not contain carbon [1].

The aim of this work is to propose a mechanism of the effect of pressure on the course of interactions during prolonged contact between alumina-mullite moulds and molten Ni-alloys.

## EXPERIMENTAL PART

Ceramic moulds were prepared by the lost wax method. The patterns ( $80 \times 20 \times 10$  mm) were immersed

into ceramic suspension of alumina containing hydrosol binder on silica base. The moulds were fired at temperature 1600 °C for three hours.

Nickel and nickel alloys of the following composition were used in this study:

- Ni-5Ti alloy (analysis: 95.47 wt.% Ni, 4.46 wt.% Ti, 0.03 wt.% Ca, 0.04 wt.% Al, < 0.03 wt.% C)
- Ni-5Cr alloy (analysis: 94.95 wt.% Ni, 4.96 wt.% Cr, 0.02 wt.% Ca, 0.03 wt.% Al, 0.05 wt.% Ti, < 0.03 wt.% C)
- ZhS6K alloy (analysis: 67.89 wt.% Ni, 10.51 wt.% Cr, 5.24 wt.% Co, 3.87 wt.% Mo, 5.27 wt.% W, 2.99 wt.% Ti, 0.16 wt.% C).

The interactions of moulds with induction-molten Ni, NiCr and NiTi were studied in Balzers vacuum furnace at temperature 1773 K for 90 minutes at Ar (or  $N_2$ ) atmosphere under pressure from  $10^{-1}$  to  $10^5$  Pa. The interactions of moulds with resistance-molten ZhS6K alloy took place in a superkanthal Heraeus furnace (type K 1700) with alumina muffle. Run time was 90 minutes at temperature 1873 K and Ar pressure from  $10^2$  to  $10^5$  Pa.

The structure of the face layers of moulds or of mould sections was studied on JXA 840A (Jeol) analytical electron microscope. The digitalized back scattered electron image was used for the analysis of the pore distribution. The volume of open pores was calculated from the mould's water absorption capacity. Bending strength was measured by three points method.

The coefficient of gas permeability was determined at temperature 1273 K by the method described in [4]. XRD analysis was used for the analysis of phase composition of the mould.

The structure and composition of the face surface of mould after interaction were studied by means of analytical electron microscopy. Mapping of chemical composition in the mould/metal interface was carried out on diagonal polished sections of moulds.

All the moulds were analyzed by means of ICP analysis at two points - on the mould face and in the depth 5 mm. Mould analyses were performed before and after interactions with Ni-alloys.

## RESULTS

### Composition and Structure of Ceramic Moulds Before Interaction with Ni-Alloys

The properties of ceramic moulds are given in Table I.

Figure 1 gives the microphotograph of the section through the mould. The dark areas represent the pores, whose size near the grains was as much as 0.5 mm. The pores were distributed irregularly on the surface as can

be seen from Figure 2, which shows the polished face surface of the mould. The pore size distribution in the face surface is given in Table II. The greater part of the pore area was made up of pores larger than 10  $\mu\text{m}$ . The overall area of pores in the face layer was over 6 %.

Table I. The properties of alumina-mullite shell moulds

volume of opened pores (vol.%)	13.32
coefficient of gas permeability at 1273 K ( $\text{m}^2$ )	$3.52 \times 10^{-13}$
chemical composition (wt.%)	Si: 2.75 Al: 49.71 O: balance
phase composition (wt.%) mullit:	21.1 $\alpha\text{-Al}_2\text{O}_3$ : balance
theoretical density ( $\text{g cm}^{-3}$ )	3.76
actual density ( $\text{g cm}^{-3}$ )	2.65
bending strength (Mpa)	54

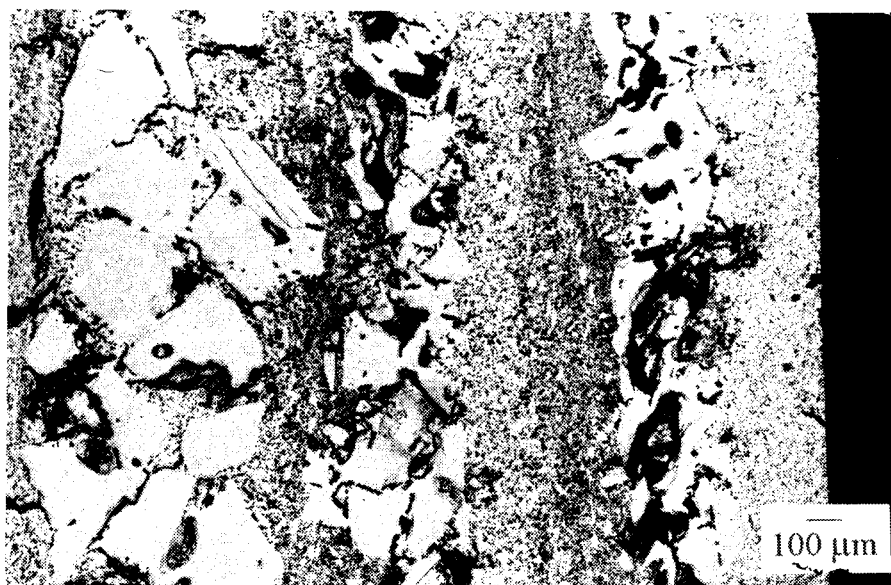


Figure 1. SEM-micrograph of the mould section before interaction

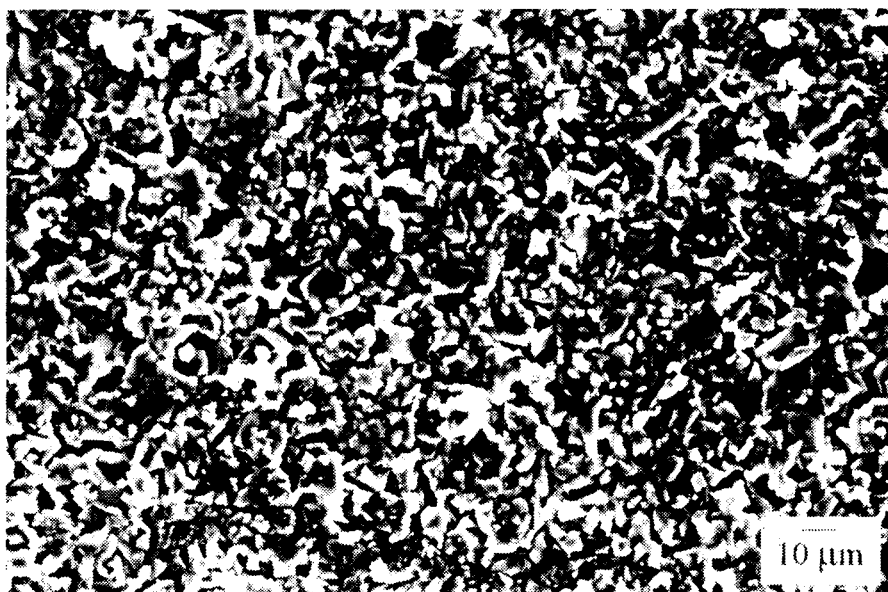


Figure 2. SEM-micrograph of the mould face surface before interaction

Table II. The pore size distribution in the face surface of alumina-mullite shell moulds

Pore size (μm)	Area of pores (% of unit area)	Number of pores per unit area
1-2	0.16	28
2-3	0.08	9
3-4	0.06	3
4-5	0.1	3
5-7	0.27	6
7-10	0.71	8
10-13	1.05	9
13-16	1.25	7
16-20	0.47	3
20-25	0.87	3
25-30	1.32	3
total	6.35	83

#### Structure of Face Surface of the Mould After Interaction with Ni and Ni-Alloys

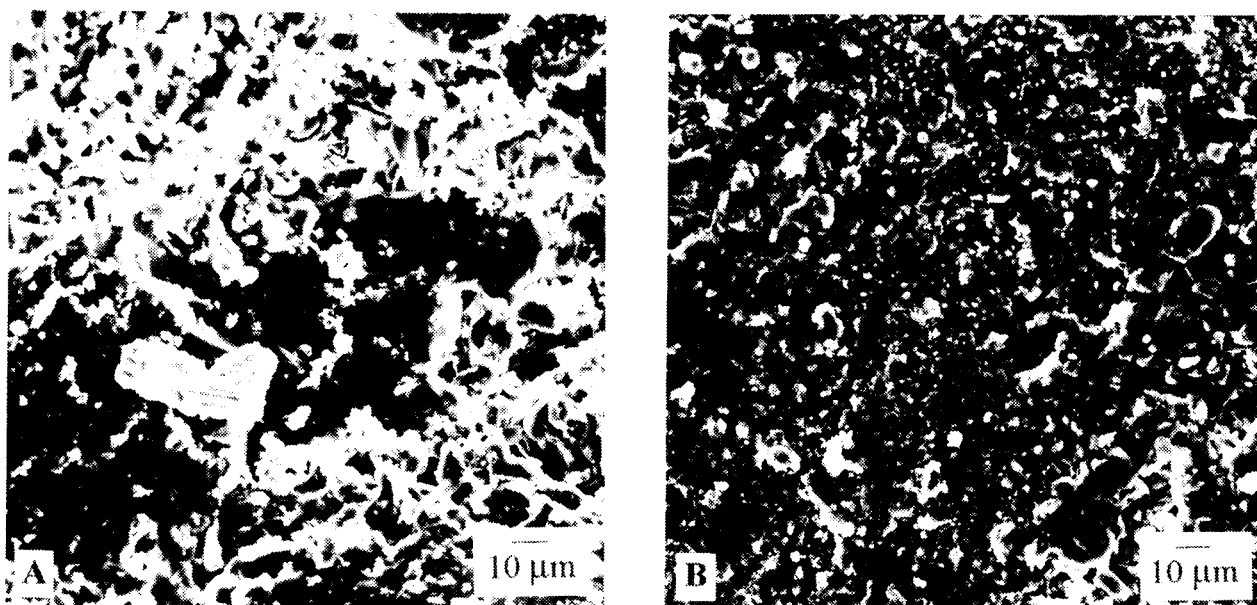
The action of molten ZhS6K alloy on the mould at temperature 1773 K and a pressure 0.15 Pa for period about 1 h resulted in the molten alloy penetration into the face layer of the mould. When the mould was cooled down, the face layer of mould penetrated with metal got stuck to the casting surface. The structure of mould surface after interaction without the face layer is seen from the microphotograph in Figure 3a. The element distribution in ceramics/alloy interface given in Figure 4a

shows the rugged surface of the mould after interaction, and the penetration of Cr, Ti and partially also Ni into the mould surface. The increase in the content of Cr, Ti and Ni, and the decrease in the content of Si in the mould surface with respect to the concentration of these elements inside the mould can be seen from Table III.

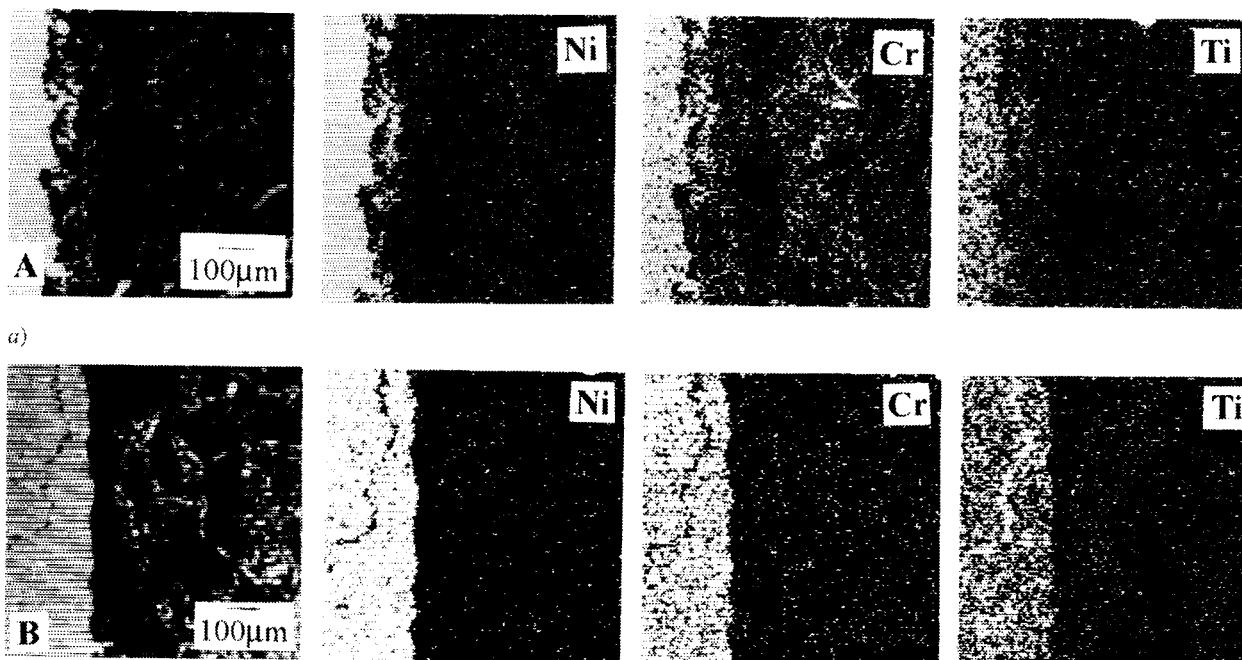
The gradual increase in the pressure of protective gas in the furnace gradually limited the penetration of molten metal into the mould surface. The erosion of the mould through the alloy could not be observed at pressure  $6 \times 10^4$  Pa of protective gas. The face layer remained compact, the casting surface was smooth. The structure of the mould surface can be seen in the microphotographs in Figure 3b.

Table III. Difference between content of elements (Cr, Ti, Ni, Si) in the face surface and in the volume of alumina-mullite moulds after interaction

alloy/pressure	Cr	Ti	Ni	Si
	(wt.%)			
ZhS6K / $6.0 \times 10^4$ Pa	+0.035	+0.015	+0.043	-
ZhS6K / $6.0 \times 10^3$ Pa	+0.265	+0.017	+0.030	-0.720
ZhS6K / $1.0 \times 10^2$ Pa	+0.502	+0.017	+0.180	-0.860
ZhS6K / $1.0 \times 10^{-1}$ Pa	+0.664	+0.017	+0.302	-1.670
Ni / $1.0 \times 10^5$ Pa	-	-	+1.690	-0.190
Ni / $1.0 \times 10^{-1}$ Pa	-	-	+2.580	-1.100
NiTi / $1.0 \times 10^5$ Pa	-	+0.31	+4.4	-
NiTi / $1.0 \times 10^{-1}$ Pa	-	+2.7	+0.356	-0.800
NiCr / $1.0 \times 10^5$ Pa	+0.466	-	+0.217	+0.220
NiCr / $1.0 \times 10^{-1}$ Pa	+0.613	-	+0.11	-1.790



a)  
Figure 3. SEM-micrograph of the face surface of alumina-mullite mould after interaction with ZhS6K alloy  
The pressure of furnace atmosphere: a) 0.15 Pa; b)  $6 \cdot 10^4$  Pa



a)  
b)  
Figure 4. The distribution of elements in alumina-mullite mould/ZhS6K interface after interaction  
The pressure of furnace atmosphere: a) 0.15 Pa; b)  $6 \cdot 10^4$  Pa

Two dimensional distribution of elements gives support to visual comparison of the ceramics/metal interface (see Figure 4b). The interface remained undamaged without significant presence of Cr, Ti and Ni in the ceramic mould.

Table III shows that the changes in Cr, Ti and Ni concentrations in the mould were not substantial. Similar effect of protective atmosphere pressure was also observed in the case of interaction of the mould with Ni, NiTi and NiCr (see Figures 5a-b to 10a-b).

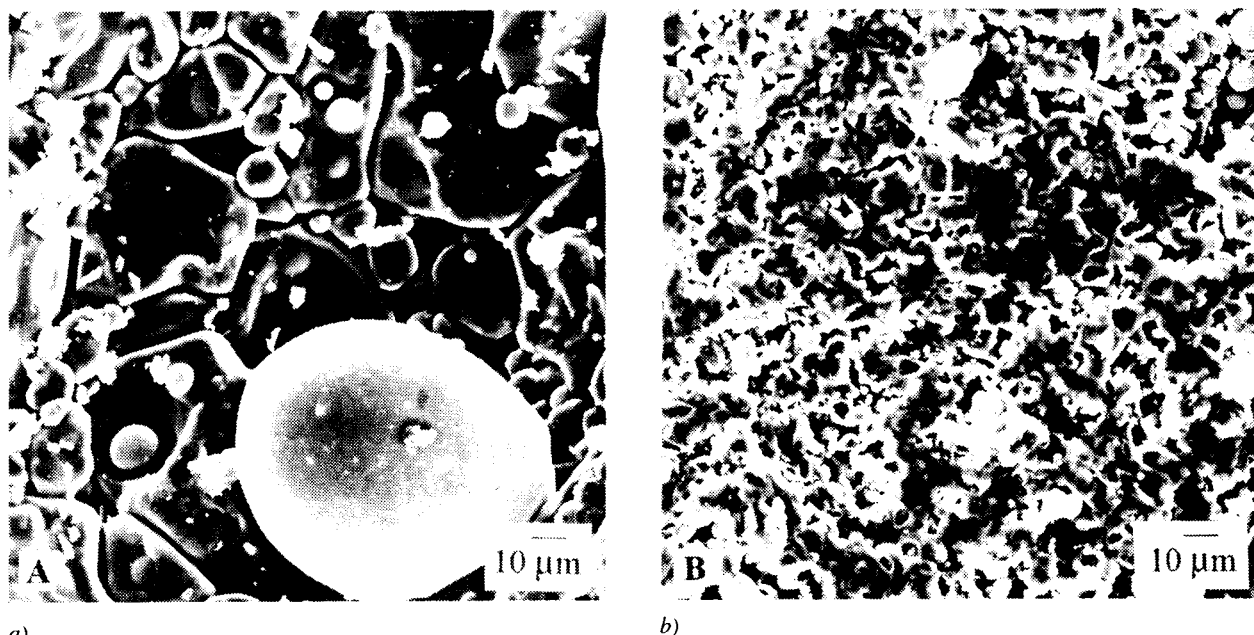


Figure 5. SEM-micrograph of the face surface of alumina-mullite mould after interaction with Ni  
The pressure of furnace atmosphere: a) 0.15 Pa ; b)  $6 \cdot 10^4$  Pa

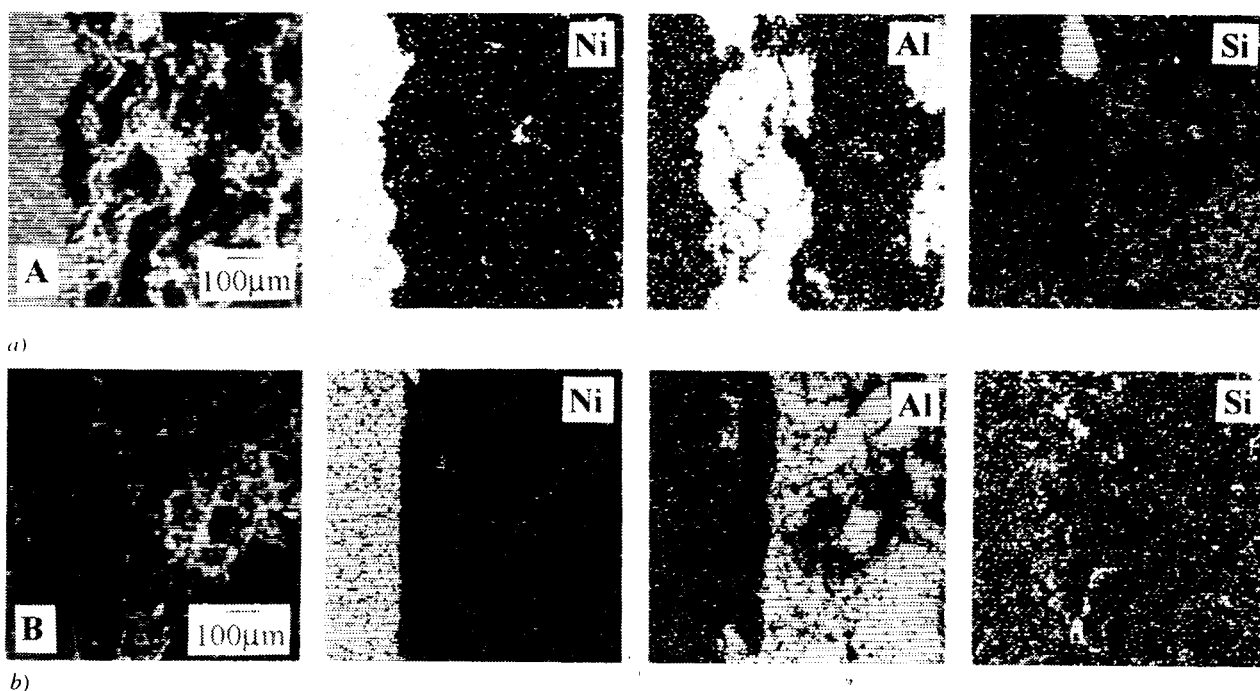


Figure 6. The distribution of elements in alumina-mullite mould/Ni interface after interaction  
The pressure of furnace atmosphere: a) 0.15 Pa; b)  $6 \cdot 10^4$  Pa

## DISCUSSION

Results have shown that the ceramic shell mould prepared by the lost wax method from fused  $\text{Al}_2\text{O}_3$  bonded with  $\text{SiO}_2$  sol contained, after firing at 1600 °C,

about 20 % mullite and 80 %  $\text{Al}_2\text{O}_3$ . No free silicon dioxide was detected in the mould. Repeated alternation of layers formed by fine particles from ceramic suspension and of layers of coarse particles of  $\text{Al}_2\text{O}_3$  from the sprinkle, on which the lost wax method is ba-

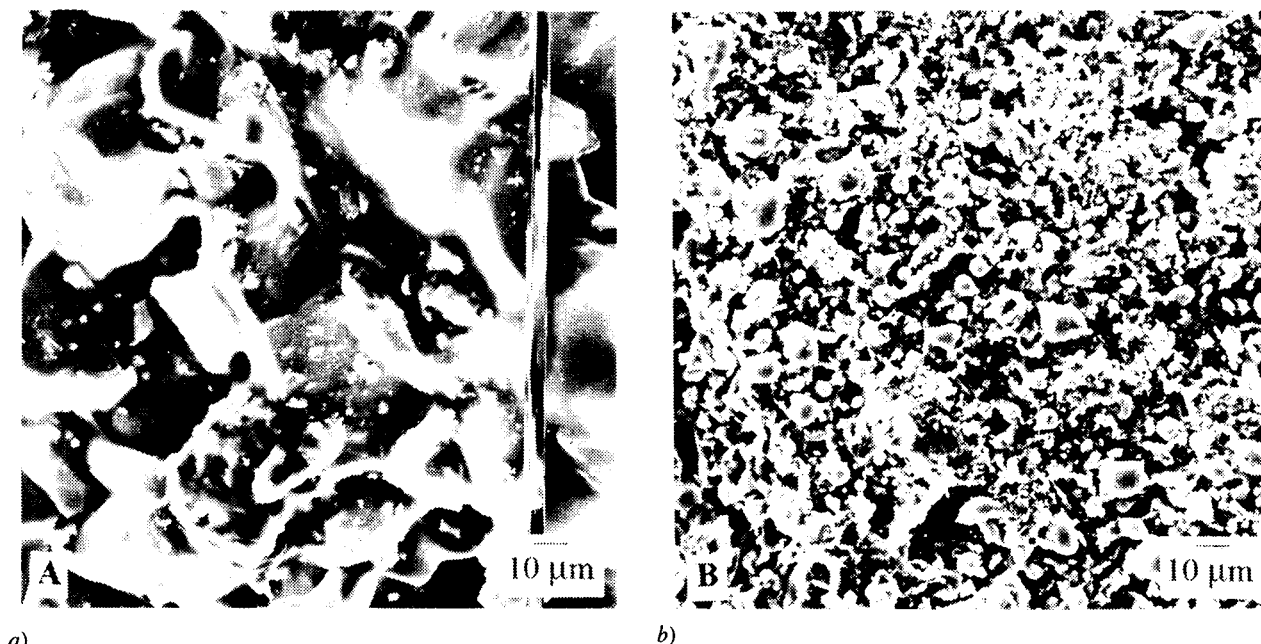


Figure 7. SEM-micrograph of the face surface of alumina-mullite mould after interaction with NiTi alloy  
The pressure of furnace atmosphere: a) 0.15 Pa; b)  $6 \cdot 10^4$  Pa

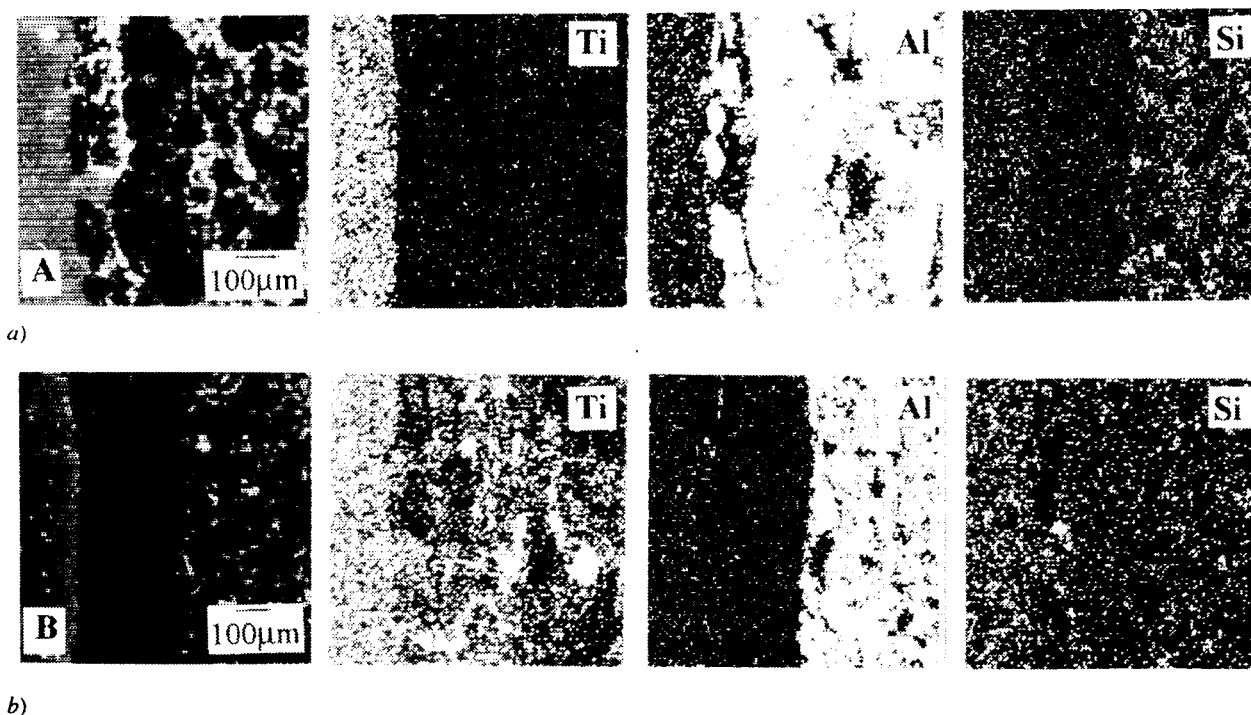


Figure 8. The distribution of the elements in the alumina-mullite mould/NiTi-alloy interface after interaction  
The pressure of furnace atmosphere: a) 0.15 Pa; b)  $6 \cdot 10^4$  Pa

sed, made it impossible to prepare a ceramic shell with closed pores. The method did not form the layer of constant thickness around the whole surface of the pattern either. The thickness of face layers in plane surfaces was from 0.3 to 0.5 mm while in corners and on

sharp edges it was half of these values. Pores on the surface of face layer were not distributed uniformly and their size was up to 30 µm. Continuous network of pores formed about 13 % of mould volume. This fact considerably affects gas permeability of the mould.

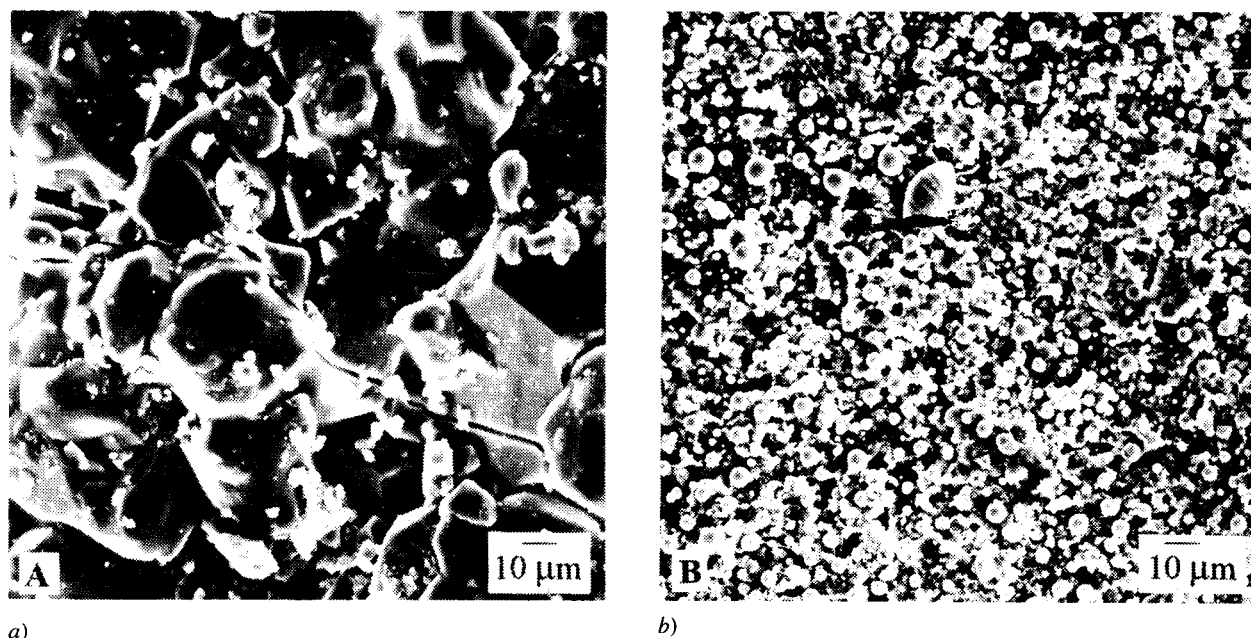


Figure 9. SEM-micrograph of the face surface of alumina-mullite mould after interaction with NiCr alloy  
The pressure of furnace atmosphere: a) 0.15 Pa; b)  $6 \cdot 10^4$  Pa

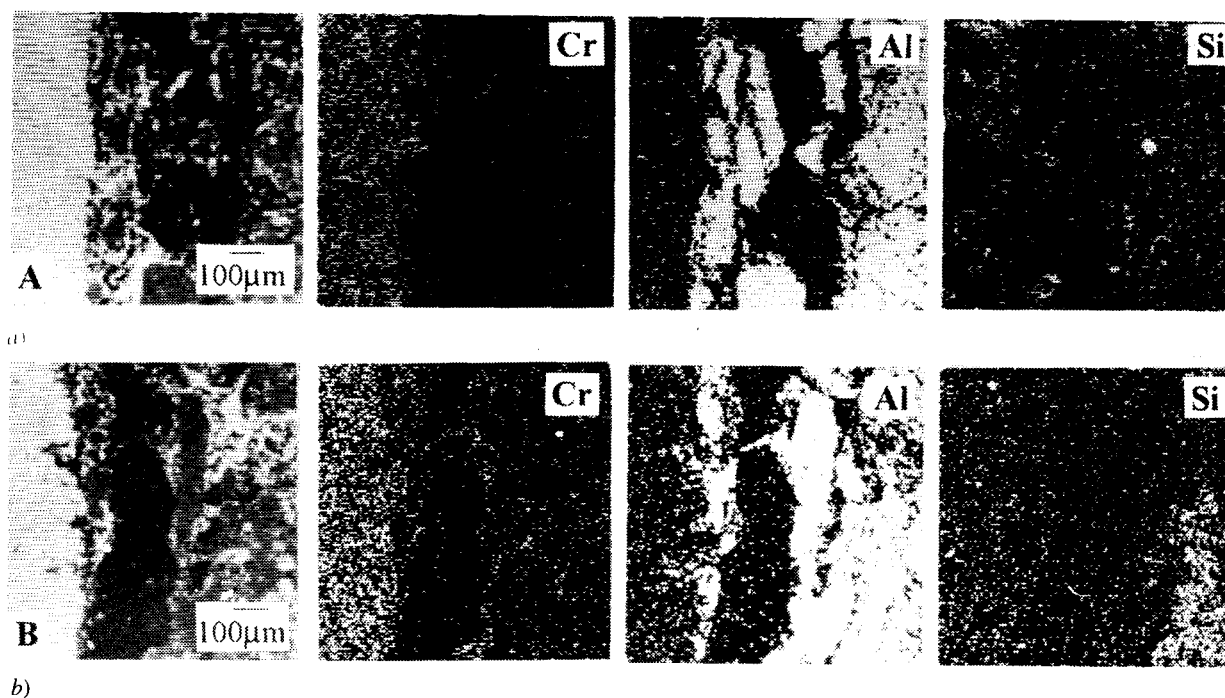


Figure 10. The distribution of the elements in the alumina-mullite mould/NiCr-alloy interface after interaction  
The pressure of furnace atmosphere: a) 0.15 Pa; b)  $6 \cdot 10^4$  Pa

The penetration of molten metal into the pores of face layer of the mould could be observed for all the Ni-alloys studied (ZhS6K, Ni-5Ti, Ni-5Cr) as well as for pure Ni. The penetration of melts into mould pores was not of purely physical nature since the surface of ceramic

materials on  $\text{Al}_2\text{O}_3$  base was not soaked with Ni-alloy melts [6]. It is only in the case of the mould surface being soaked with alloys or if the metallostatic pressures are sufficiently high that the molten alloy could penetrate into mould pores by physical means. The penetration of

molten alloys into mould pores was therefore affected by physical-chemical processes.

Considerable increase in the penetration of melts into mould pores was observed with reducing the pressure of protective atmosphere for all the Ni-alloys studied as well as for pure Ni. The erosion activity of the molten metals under study increased in the order:



It can be assumed that pressure affected especially physical and chemical processes between alloys and the mould in which the substances participated in gaseous phase. Interactions on the  $\text{Al}_2\text{O}_3$  / Ni-alloy interface (and the accompanying decrease in surface tension) with reduced pressure in the furnace could be observed, for example, in Ni-alloys containing carbon [2].

Table IV gives hypothetical chemical reactions between the components of ceramic mould (mullite and  $\text{Al}_2\text{O}_3$ ) and selected reactive pure components of the alloys studied (Ni, Cr, Ti and C).

Figure 11 presents the temperature dependencies of standard reaction Gibbs energies for reactions given in Table IV. It can be seen from the values of  $\Delta_r G_T^0$  that in

the direction of expected products only reactions (1) to (5) can take place spontaneously at normal pressure and at 1800 K, i.e. reactions of titanium with mullite. With the exception of equation (5), none of the above reactions gives rise to volatile gaseous products of the type  $\text{TiO(g)}$ ,  $\text{SiO(g)}$  or  $\text{Al}_2\text{O(g)}$ . The reduced pressure will act in the direction of forming the above products and will shift the balance to the right, especially in the case of equations (10) and (11). This shift, however, will not be very pronounced and it cannot fully explain the results observed. The penetration of molten Ni-alloys and erosion of moulds at low pressure has thus also other causes. Figure 12 gives in graphic form the dependence of saturated vapour pressure on temperature for the elements that were part of the Ni-alloys (Ni, Ti, Cr, Al) or Si resulted from reactions (1) - (4). At temperature 1800 K the vapour pressure for Ni is 1.26 Pa, for Cr 9.18 Pa, for Ti 0.0556 Pa, for Al 81.3 Pa, and for Si 0.221 Pa. Since these values are given for pure components, the partial pressures of alloy components, excepting Ni, will be lower. In the case of Ni, activity is around one (in Ni and in the alloys Ni-5Ti and Ni-5Cr) and its intensive evaporation can be expected especially at pressure below 1 Pa.

Table IV. Hypothetical reactions of alumina and mullite with pure Ti, Ni, Cr and C at standard conditions

1.	1/4 mullite(s) + Ti(s,l)	$\rightleftharpoons$	3/4 $\text{Al}_2\text{O}_3(\text{s})$ + 1/2 $\text{Si}(\text{s,l})$ + $\text{TiO}(\text{g})$
2.	3/8 mullite(s) + Ti(s,l)	$\rightleftharpoons$	9/8 $\text{Al}_2\text{O}_3(\text{s})$ + 3/4 $\text{Si}(\text{s,l})$ + 1/2 $\text{Ti}_2\text{O}_3(\text{s})$
3.	5/12 mullite(s) + Ti(s,l)	$\rightleftharpoons$	5/4 $\text{Al}_2\text{O}_3(\text{s})$ + 5/6 $\text{Si}(\text{s,l})$ + 1/3 $\text{Ti}_3\text{O}_5(\text{s})$
4.	1/2 mullite(s) + Ti(s,l)	$\rightleftharpoons$	3/2 $\text{Al}_2\text{O}_3(\text{s})$ + $\text{Si}(\text{s,l})$ + $\text{TiO}_2(\text{s})$
5.	1/2 mullite(s) + Ti(s,l)	$\rightleftharpoons$	3/2 $\text{Al}_2\text{O}_3(\text{s})$ + $\text{SiO}(\text{g})$ + $\text{TiO}(\text{g})$
6.	1/2 $\text{Al}_2\text{O}_3(\text{s})$ + Ti(s,l)	$\rightleftharpoons$	$\text{Al}(\text{l})$ + 1/2 $\text{Ti}_3\text{O}_5(\text{s})$
7.	5/9 $\text{Al}_2\text{O}_3(\text{s})$ + Ti(s,l)	$\rightleftharpoons$	10/9 $\text{Al}(\text{l})$ + $\text{Ti}_3\text{O}_5(\text{s})$
8.	3/8 mullite(s) + Cr(s,l)	$\rightleftharpoons$	9/8 $\text{Al}_2\text{O}_3(\text{s})$ + 3/4 $\text{Si}(\text{s,l})$ + 1/2 $\text{Cr}_2\text{O}_3(\text{s})$
9.	2/3 $\text{Al}_2\text{O}_3(\text{s})$ + Ti(s,l)	$\rightleftharpoons$	4/3 $\text{Al}(\text{l})$ + $\text{TiO}_2(\text{s})$
10.	1/4 mullite(s) + C(s,l)	$\rightleftharpoons$	3/4 $\text{Al}_2\text{O}_3(\text{s})$ + 1/2 $\text{Si}(\text{s,l})$ + $\text{CO}(\text{g})$
11.	3/4 mullite(s) + Ti(s,l)	$\rightleftharpoons$	9/4 $\text{Al}_2\text{O}_3(\text{s})$ + 3/2 $\text{SiO}(\text{g})$ + 1/2 $\text{Ti}_2\text{O}_3(\text{s})$
12.	5/6 mullite(s) + Ti(s,l)	$\rightleftharpoons$	5/2 $\text{Al}_2\text{O}_3(\text{s})$ + 5/3 $\text{SiO}(\text{s})$ + 1/3 $\text{Ti}_3\text{O}_5(\text{s})$
13.	3/4 $\text{Al}_2\text{O}_3(\text{s})$ + Ti(s,l)	$\rightleftharpoons$	3/4 $\text{Al}_2\text{O}(\text{g})$ + 1/2 $\text{Ti}_2\text{O}_3(\text{s})$
14.	1/4 mullite(s) + Ni(s,l)	$\rightleftharpoons$	3/4 $\text{Al}_2\text{O}_3(\text{s})$ + 1/2 $\text{Si}(\text{s,l})$ + $\text{NiO}(\text{s})$
15.	5/6 $\text{Al}_2\text{O}_3(\text{s})$ + Ti(s,l)	$\rightleftharpoons$	5/6 $\text{Al}_2\text{O}(\text{g})$ + 1/3 $\text{Ti}_3\text{O}_5(\text{s})$
16.	mullite(s) + Ti(s,l)	$\rightleftharpoons$	3 $\text{Al}_2\text{O}_3(\text{s})$ + 2 $\text{SiO}(\text{g})$ + $\text{TiO}_2(\text{s})$
17.	1/2 mullite(s) + C(s,l)	$\rightleftharpoons$	3/2 $\text{Al}_2\text{O}_3(\text{s})$ + $\text{SiO}(\text{g})$ + $\text{CO}(\text{g})$
18.	3/4 mullite(s) + Cr(s,l)	$\rightleftharpoons$	9/4 $\text{Al}_2\text{O}_3(\text{s})$ + 3/2 $\text{SiO}(\text{g})$ + 1/2 $\text{Cr}_2\text{O}_3(\text{s})$
19.	$\text{Al}_2\text{O}_3(\text{s})$ + Ti(s,l)	$\rightleftharpoons$	$\text{Al}_2\text{O}(\text{g})$ + $\text{TiO}_2(\text{s})$
20.	1/2 mullite(s) + Ni(s,l)	$\rightleftharpoons$	3/2 $\text{Al}_2\text{O}_3(\text{s})$ + $\text{SiO}(\text{g})$ + $\text{Ni}(\text{s,l})$



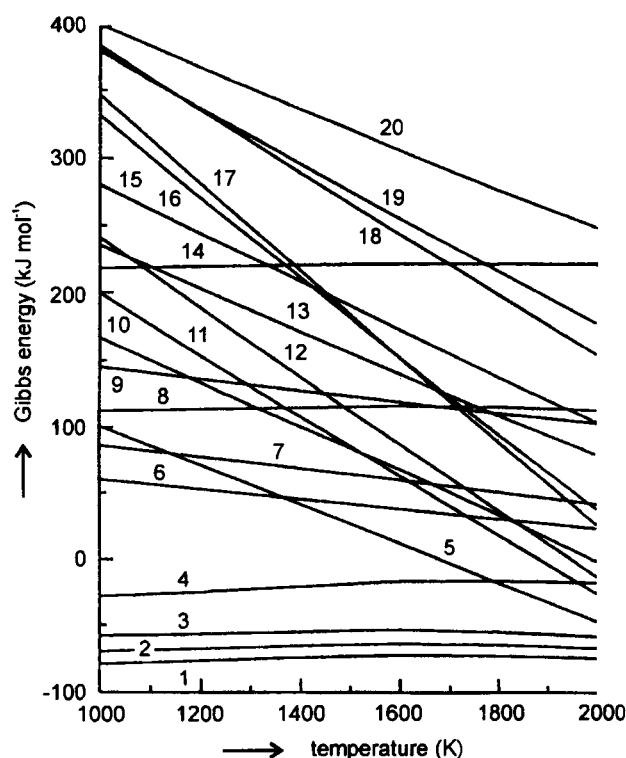


Figure 11. The temperature dependence of the standard Gibbs energy of hypothetical reactions between alumina or mullite and Ni, Ti, Cr and C (see Table IV)

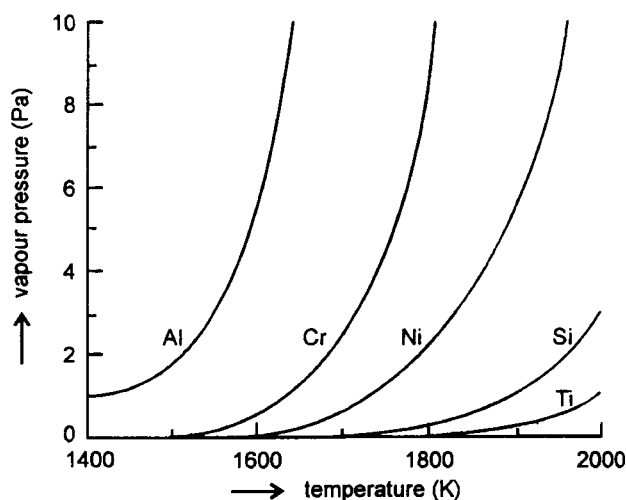


Figure 12. The temperature dependence of saturated vapour pressure of Ni, Ti, Cr, Al and Si

The results given in the preceding chapter and the assumptions made in the discussion make it possible to propose a mechanism of interaction of alumina-mullite moulds with molten Ni and its alloys at reduced pressure in these points:

1. Alumina-mullite shell mould has a porous structure that is permeable especially by substances in gaseous phase.
2. The alloy components (especially Ni) are evaporated at low pressure not only on the molten Ni-alloy/furnace atmosphere interface but also on the molten Ni-alloy/mould ceramic one. Pressure difference between the mould/alloy surface and the outer mould surface accelerates evaporation of the alloy component into the mould pores.
3. The reactive components in alloys (Ti, Cr, Ni) get into direct contact with the mould ceramics, which facilitates the reaction between alloy components and ceramic mould ones. It is especially Ti that reacts with mullite, namely with silicon dioxide. The gaseous reaction products are Si(g) and SiO(g). The reaction of Cr with mould ceramic is aided by the dissolving of the reaction product ( $\text{Cr}_2\text{O}_3$  or  $\text{Cr}^{3+}$ ) in  $\text{Al}_2\text{O}_3$ . Pure Ni penetrates into the mould above all through evaporation. Chemical reactions taking place on the ceramic/alloy interface result in a change of its composition (the interface is enriched especially with  $\text{Ti}^{3+}$  and  $\text{Cr}^{3+}$  oxides) and the interface becomes wettable.
4. The pores eroded by chemical reactions become gradually wider and the alloy penetrates into the pores. The process of penetration is enhanced by the pressure gradient between the inner and outer wall of the mould.
5. When the mould is cooled, the alloy solidifies in the mould pores and the ceramic soaked with metal gets stuck on the surface of the casting.

The scheme of the penetration mechanism which was described in the previous text is given in the Figure 13.

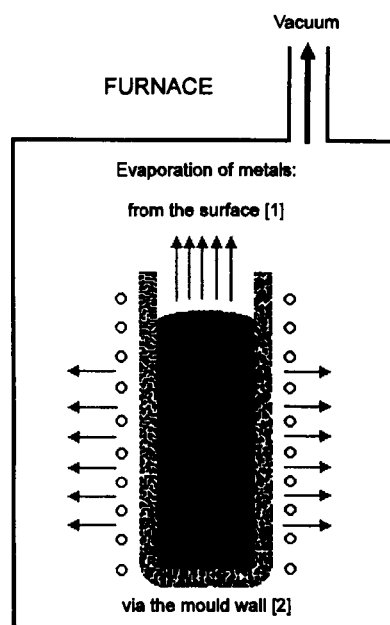


Figure 13. Evaporation of metallic components of alloys in the course of interaction experiment

## CONCLUSION

Unidirectional solidification of Ni-alloys in alumina-mullite moulds at protective gas pressures above  $10^4$  Pa yields casting surfaces of higher quality than solidification under high vacuum.

## Acknowledgement

This work was supported by Czech COST program.

## References

1. Cihlář J., Horáček M.: Proc. 21st European Conference on Investment Casting, Lugano 1990. Paper No.6.
2. Snape E., Beeley P.R.: J. Am. Ceram. Soc. 50, 349 (1967).
3. Huseby I.C., Klug F.J.: Am. Ceram. Soc. Bull. 58, 527 (1979).
4. CS patent No.: 228671.
5. Armstrong W.M. and all: J. Am. Ceram. Soc. 45, 115 (1962).
6. Kubaschewski O., Alcock C.B.: *Metallurgical Thermochemistry*, Pergamon Press, Oxford 1979.
7. Barin I., Knacke O.: *Thermochemical Properties of Inorganic Substances*, Springer-Verlag, Berlin 1973.

*Submitted in English by the authors*

## VLIV TLAKU NA INTERAKCI KORUND-MULITOVÝCH FOREM S TAVENINAMI NIKLOVÝCH SLITIN

JAROSLAV CIHLÁŘ, KAREL MACA, PETER MARQUIS\*

*Ústav materiálového inženýrství, odbor keramiky,  
Vysoké učení technické v Brně, Technická 2, 616 69 Brno  
\*University of Birmingham, Great Britain*

Interakce skořepinových korund-mulitových forem s taveninami niklu a jeho slitin (Ni, Ni-Cr, Ni-Ti, ŽS6K) při nízkém tlaku ( $1$  až  $10^3$  Pa) byla popsána v těchto bodech:

1. Skořepinová forma měla porézní strukturu, která byla prostupná zejména pro látky v plynné fázi. Při nízkém tlaku v peci docházelo, v důsledku tlakového spádu mezi lícním a vnějším povrchem skořepinové formy, k odpařování složek slitin (zejména Ni) do pórů v lícním povrchu formy.
2. Reaktivní složky (zejména Ti, Cr) se tak dostávaly do přímého kontaktu s keramikou formy, což usnadnilo chemické reakce mezi složkami slitin a složkami keramické formy. Ti reagoval s mulitem za vzniku plynných reakčních produktů Si(g), SiO(g) resp. Ti(g). Nízký tlak v peci usnadňoval tvorbu těchto reakčních produktů. Reakce Cr s keramikou formy byla podporována rozpouštěním reakčního produktu  $\text{Cr}_2\text{O}_3$  v  $\text{Al}_2\text{O}_3$ .  
Chemické reakce probíhající na rozhraní slitina/keramika vedly ke změně chemického složení rozhraní (rozhraní bylo obohaceno zejména oxidy  $\text{Ti}^{3+}$  a  $\text{Cr}^{3+}$ ) a to se stávalo smáčivé. Póry byly chemickými reakcemi erodovány a postupně se zvětšovaly. Obě změny, zvýšení smáčivosti a rozšiřování pórů usnadňovaly penetraci slitiny do pórů keramiky.
3. Zvýšení tlaku ochranné pecní atmosféry nad  $10^4$  Pa prakticky zabránilo penetraci a erozi lícního povrchu forem taveninami niklových slitin.